Geophysical Journal International

Geophys. J. Int. (2011) **186,** 221–225 doi: 10.1111/j.1365-246X.2011.05064.x

EXPRESS LETTER

A theory for microtremor *H*/*V* spectral ratio: application for a layered medium

Francisco J. Sánchez-Sesma,[1] Miguel Rodríguez,[1] Ursula Iturrarán-Viveros,[2] Francisco Luzón,[3] Michel Campillo,[4] Ludovic Margerin,[5] Antonio García-Jerez,[3] Martha Suarez,[1] Miguel A. Santoyo[6] and Alejandro Rodríguez-Castellanos[7]

[1]*Instituto de Ingeniería, Universidad Nacional Autónoma de México, C.U., Coyoacán* 04510 *D.F., Mexico*
[2]*Facultad de Ciencias, Universidad Nacional Autónoma de México, C.U., Coyoacán* 04510 *D.F., Mexico*
[3]*Depto. Física Aplicada, U. Almería, Cañada de San Urbano s/n,* 04120-*Almería, Spain. E-mail: fluzon@ual.es*
[4]*LGIT, Observatoire de Grenoble, Université Joseph Fourier, B.P.* 5, 38041 *Grenoble Cede, France*
[5]*Observatoire Midi-Pyrénées, CNRS UMR* 5562, 14, *Avenue Edouard Belin,* 31400 *Toulouse, France*
[6]*Depto. Geofísica y Meteorología, Facultad Ciencias Físicas, Cd. Universitaria,* 28040 *Madrid, Spain*
[7]*Instituto Mexicano del Petróleo, L. Cárdenas* 152, 07730 *D.F., Mexico*

Accepted 2011 April 27. Received 2011 April 27; in original form 2010 June 2

SUMMARY

Microtremors are produced by multiple random sources close to the surface of the Earth. They may include the effects of multiple scattering, which suggests that their intensities could be well described by diffusion-like equations. Within this theoretical framework, the average autocorrelation of the motions at a given receiver, in the frequency domain, measures average energy density and is proportional to the imaginary part of the Green's function (GF) when both source and receiver are the same.

Assuming the seismic field is diffuse we compute the *H*/*V* ratio for a surface receiver on a horizontally layered medium in terms of the imaginary part of the GF at the source. This theory links average energy densities with the GF in 3-D and considers the *H*/*V* ratio as an intrinsic property of the medium. Therefore, our approach naturally allows for the inversion of *H*/*V*, the well-known Nakamura's ratio including the contributions of Rayleigh, Love and body waves. Broad-band noise records at Texcoco, a soft soil site near Mexico City, are studied and interpreted using this theory.

Key words: Inverse theory; Earthquake ground motions; Coda waves; Site effects; Statistical seismology; Wave scattering and diffraction.

GJI Seismology

1 INTRODUCTION

Site conditions can generate significant changes in earthquake ground motion producing concentrated damage (Sánchez-Sesma 1987; Aki 1988). It is usual to characterize the site effects by means of spectral ratios of recorded motions with respect to reference rock site (e.g. Cadet *et al*. 2010). These ratios are called empirical transfer functions (ETF), and for seismically active locations can be easily obtained. It is often appropriate to interpret the ETF assuming a 1-D configuration and deal with resonant frequencies and amplifications. By means of logging or seismic surveys the 1-D soil structure can be obtained allowing for simple theoretical transfer functions.

On the other hand, for more quiescent areas seismic noise may provide useful information. In fact, Lermo & Chávez-García (1994) obtained reliable estimates of the soil resonance frequencies from the spectral ratio between horizontal and vertical motions of microtremors. The noise *H*/*V* spectral ratio (NHV) has been studied to explain its strengths and limitations (Bonnefoy-Claudet *et al.* 2006; Cadet 2007; Bard 2008; Pilz *et al.* 2009; Lunedei & Albarello 2010). Usually the NHV reveals the site dominant frequency f_0 but the amplitude of the NHV is not well understood (Pilz *et al*. 2009). The recent work of Lunedei & Albarello (2010) is a significant step towards the understanding of the NHV. They computed the field at a given location considering a continuous distribution of random sources at the surface of a weakly dissipative layered system.

The ratio *H*/*V* became a puzzle and several proposals exist to interpret its features. For instance, it was assumed that microtremors were mainly composed of surface waves. In fact, the ratio *H*/*V* has been related to Rayleigh wave ellipticity (Lermo & Chávez-García 1994; Malischewsky & Scherbaum 2004). When Rayleigh and Love waves come from various directions an ellipticity analysis

becomes very complicated. However, successful inversion schemes based on surface wave ellipticity have been used (Arai & Tokimatsu 2004; Cadet 2007). On the other hand, other authors claim for the dominance of body waves around the peak of the H/V (see e.g. Nakamura 2000; Bonnefoy-Claudet *et al.* 2008; Herat 2008).

Here we assume that the noise is a diffuse wavefield containing all types of elastic waves. This may provide deep physical insight and explain the success of one of the most used techniques nowadays. Underlying this assumption is the connection between diffuse fields and the Green's function (GF, Campillo & Paul 2003; Weaver & Lobkis 2004; Sánchez-Sesma & Campillo 2006; Sánchez-Sesma *et al*. 2008; Yokoi & Margaryan 2008; Sato 2010), which implies the proportionality between the average energy densities of a diffuse field and the imaginary part of GF at the source (Sánchez-Sesma *et al.* 2008; Perton *et al.* 2009). Thus, we express the NHV as the square root of the ratio of the corresponding imaginary parts of Green's tensor components (Sánchez-Sesma *et al.* 2010). We use this theory to explain results from an experiment at Texcoco, a site near Mexico City within the ancient lake bed.

2 DIFFUSE FIELDS IN DYNAMIC ELASTICITY

Consider an elastic inhomogeneous, anisotropic medium subjected to a set of uncorrelated random forces. The correlation properties of the resulting field and of a multiple-scattered wavefield are equivalent. Since the latter are well described by diffusion-like equations, we employ the term 'diffuse' for the noise wavefield. In this case, the GF can be retrieved from averaging cross correlations of the recorded motions (Campillo & Paul 2003; Sánchez-Sesma *et al.* 2008).

For a diffuse field we can establish that the 'average autocorrelation' of motion for a given direction at a given point is proportional to the 'directional energy density' (DED). Thus, the energy densities at given directions are proportional to the imaginary part of GF tensor components at such point. The relationships among energy densities and their partitions have been recently studied by Perton *et al*. (2009) and by Margerin *et al.* (2009). This concept of the directional energy densities has been explored further and the connection between deterministic results (regarding energy partitions in a half-space due to surface loads) and diffuse fields has been clearly established (Sánchez-Sesma *et al.* 2011).

3 THE RETRIEVAL OF THE GF FROM CORRELATIONS

It has been demonstrated (Perton *et al.* 2009) that if a 3-D diffuse, equipartitioned, harmonic displacement vector field $u_i(\mathbf{x}, \omega)$ is established within an elastic medium, the average cross correlations of motions at points $\mathbf{x_A}$ and $\mathbf{x_B}$ can be written as

$$\left\langle u_i(\mathbf{x_A}, \omega) u_j^*(\mathbf{x_B}, \omega) \right\rangle = -2\pi E_S k^{-3} \mathrm{Im}[G_{ij}(\mathbf{x_A}, \mathbf{x_B}, \omega)], \tag{1}$$

where the GF $G_{ij}(\mathbf{x_A}, \mathbf{x_B}, \omega)$ = displacement at $\mathbf{x_A}$ in direction i produced by a unit harmonic load acting at $\mathbf{x_B}$ in direction $j = \delta_{ij}\delta(|\mathbf{x} - \mathbf{x_B}|)\exp(\mathrm{i}\omega t)$, $\mathrm{i} = \sqrt{-1}$ = imaginary unit, ω = circular frequency, t = time, $k = \omega/\beta$ = shear wave number, β = shear wave propagation velocity, $E_S = \rho\omega^2 S^2$ = average energy density of shear waves which is a measure of the strength of the diffuse illumination, ρ = mass density and S^2 = average spectral density of shear waves. The asterisk ($*$) means the complex conjugate and the angular brackets denote azimuthal average. Eq. (1) is the analytical consequence of a correlation-type elastic representation theorem and has been verified in canonical examples of a full space (Sánchez-Sesma & Campillo 2006) and for inclusions (Sánchez-Sesma *et al*. 2006, 2008).

4 ENERGY DENSITIES AT GIVEN POINTS AND DIRECTIONS

The energy density at point $\mathbf{x_A}$ can be obtained if we rewrite eq. (1) assuming $\mathbf{x_A} = \mathbf{x_B}$.

$$\begin{aligned} E(\mathbf{x_A}) &= \rho\omega^2 \left\langle u_m(\mathbf{x_A}) u_m^*(\mathbf{x_A}) \right\rangle \\ &= -2\pi\mu E_S k^{-1} \mathrm{Im}[G_{mm}(\mathbf{x_A}, \mathbf{x_A})]. \end{aligned} \tag{2}$$

The total energy density at a point is proportional to the imaginary part of the trace of the Green's tensor for coincident receiver and source. The imaginary part represents the power injected by the unit harmonic load. This quantity 'detects' energies that are both radiated and coming back to the source and may be used for imaging. Eq. (2) is valid even if the summation convention is ignored (Perton *et al*. 2009). In that case $E(\mathbf{x_A}) \equiv E_m(\mathbf{x_A})$ = DED along direction m.

5 THE TWO FACES OF EQUIPARTITION

Equipartition is a first principle. Generally we cannot observe it directly but we can infer its reality after realizing its consequences. Within an infinite, homogeneous elastic medium (Weaver 1982, 1985; Perton *et al*. 2009) a diffuse field displays energy densities along any direction with one-third of the available energy. This is 'classical' equipartition in terms of degrees of freedom. Alternatively, equipartition can be invoked for wave modes. Weaver (1982) showed that the ratio of shear and dilatational energy densities is $2\alpha^3/\beta^3$, where α = velocity of P waves. Therefore, the energy fractions of available energy density for shear and compressional waves are $2R^3/(1 + 2R^3)$ and $1/(1 + 2R^3)$, respectively, where $R = \alpha/\beta$. Let us call this 'elastic' equipartition.

Although for the full space the equivalence between classical and elastic equipartition is trivial, in a half-space this is somehow more complicated but it has already been established (Weaver 1985; Perton *et al.* 2009). In the real Earth it is difficult to observe equipartition explicitly. It has been pointed out in the coda of earthquakes from detailed array analysis (Margerin *et al.* 2009).

6 THE NHV

Assume that a seismic field of microtremors is diffuse. We interpret the stabilized spectral densities as DEDs. We can thus write the H/V ratio as

$$[H/V](\omega) = \sqrt{\frac{E_1(\mathbf{x}, \omega) + E_2(\mathbf{x}, \omega)}{E_3(\mathbf{x}, \omega)}}, \tag{3}$$

where E_1, E_2 and E_3 are the DEDs and the subscripts 1 and 2 refer to horizontal, and 3 to vertical degrees of freedom. This is essentially the definition given by Arai & Tokimatsu (2004). To interpret the NHV a primary ingredient has been the ellipticity of Rayleigh waves (Lermo & Chávez-García 1994; Fäh *et al.* 2001; Arai & Tokimatsu 2004).

Here, we express the NHV in terms of DEDs of a diffuse field that are then proportional to the imaginary part of the GF at the source (for a discussion, see Sánchez-Sesma *et al.* 2008; Perton

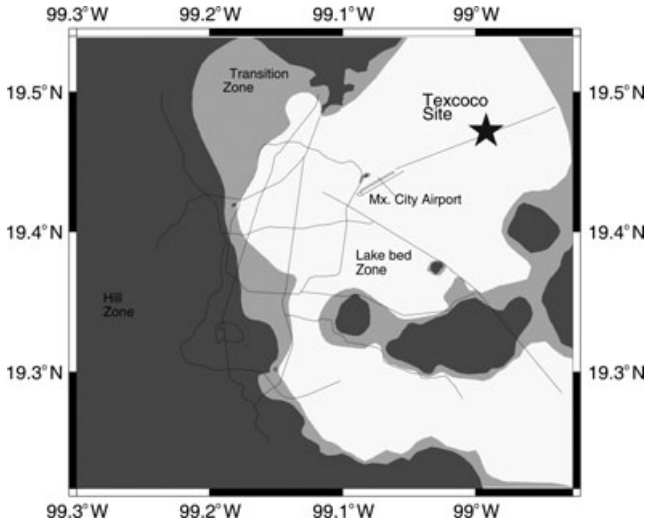

Figure 1. Geotechnical map of Mexico City. The three zones that characterize the region are depicted: I, Firm Ground; II, Transition and III, Lakebed zones.

et al. 2009). Let's consider eqs (2) and (3) and write

$$[H/V](\omega) = \sqrt{\frac{\mathrm{Im}[G_{11}(\mathbf{x},\mathbf{x};\omega)] + \mathrm{Im}[G_{22}(\mathbf{x},\mathbf{x};\omega)]}{\mathrm{Im}[G_{33}(\mathbf{x},\mathbf{x};\omega)]}}. \quad (4)$$

This equation (Sánchez-Sesma *et al.* 2010) links 'average' measurements expressed on the left-hand side with an *intrinsic* property of the medium on the right-hand side, and naturally allows for the inversion of H/V, the Nakamura's ratio accounting for the contributions of Rayleigh, Love and body waves.

7 THE TEXCOCO EXPERIMENT

A broad-band station with a fundamental period sensor of $T_0 = 30$ s was used to record microtremors at the Texcoco lakebed at a site close to Mexico City (Fig. 1), a flat zone with a clay layer. Our data consist of noise records of approximately 6.4 hr in three components. The normalization criterion consists in dividing each component by the square root of the sum of autocorrelations for the three components, integrated in frequency. This guarantees that the associated total energy for each window is equal. In the 'Supplementary Information' results for several window lengths and number of windows are shown. A remarkable characteristic of the noise we recorded at Texcoco is the consistency of spectral measurements. In our analysis we use windows of 40 s that give reliable spectral estimates for frequencies larger than 0.3 Hz (i.e. more than about 12 cycles per window). Fig. 2 displays normalized autocorrelations or spectral densities.

8 A LAYERED MEDIUM OVER HALF-SPACE: 3-D SOLUTION

Consider a stack of N parallel elastic layers, with thickness h_j, compressional and shear velocities α_j and β_j, mass density ρ_j and quality factor Q_j ($j = 1, \ldots, N$) overlaying a half-space (for $j = N + 1$) as depicted in Fig. 3. Interfaces allow continuity of displacements and tractions and free boundary conditions of null tractions at the top, except for concentrated vector unit point loads at the surface.

A formulation that uses a generalized modal superposition has been recently proposed (Margerin 2009) to compute energy ratios.

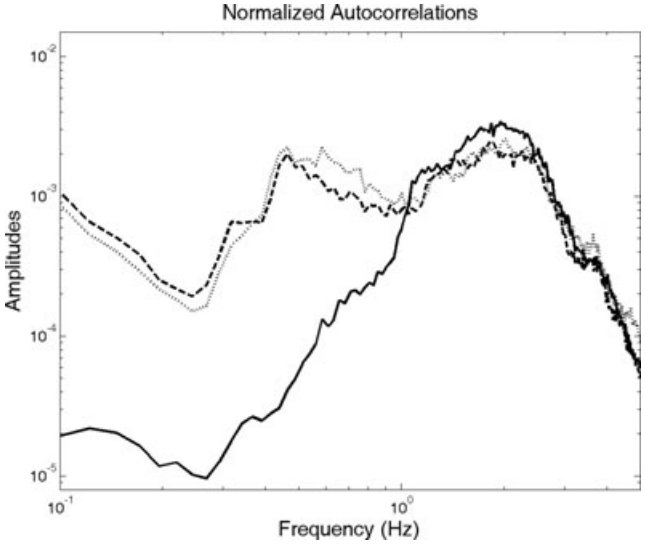

Figure 2. Normalized average autocorrelations of horizontal and vertical motion at the Texcoco site. Vertical and horizontal (NS and EW) motions are represented with continuous and dashed lines, respectively. Duration of windows is 40 s. For details see the Supplementary Information.

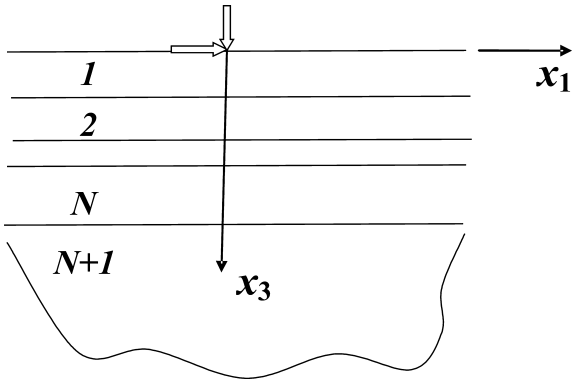

Figure 3. Stack of N parallel elastic layers over a 3-D half-space.

In this work we used also standard methods based upon potentials (e.g. Knopoff 1964) to obtain explicitly the Green's tensor as integrals in the radial wavenumber domain. These two approaches are equivalent. Details are given in the Supplementary Information.

9 MODELLING IN 3-D AND NOISE *H/V* SPECTRA

To provide a preliminary explanation of the Texcoco data we assumed a simplified model composed of a single layer of thickness $H = 40$ m, S-wave velocity $\beta = 70$ m s^{-1}, mass density $\rho = 1.2$ g cm^{-3} and quality factor $Q = 100$. Regarding the P-wave velocity two extreme values were selected $\alpha = 400$ and 800 m s^{-1}. These values correspond to Poisson ratios of 0.4842 and 0.4961, respectively. Several tests reveal P waves have little influence on results. The values assumed for the half-space are $\alpha = 2000$ m s^{-1}, $\beta = 1000$ m s^{-1} and $\rho = 2.5$ g cm^{-3}. A complete parametric analysis is a matter of our current research but is beyond the scope of this communication. Fig. 4 shows the results for horizontal and vertical loads. The stair-like character of $\mathrm{Im}G_{11}$ reveals 'shear resonances'. The behaviour of $\mathrm{Im}G_{33}$ is different. It displays a peak at 1 Hz as the result of interacting P and S waves and is dominated by the 'emission' of Rayleigh waves at high frequencies. This interpretation is

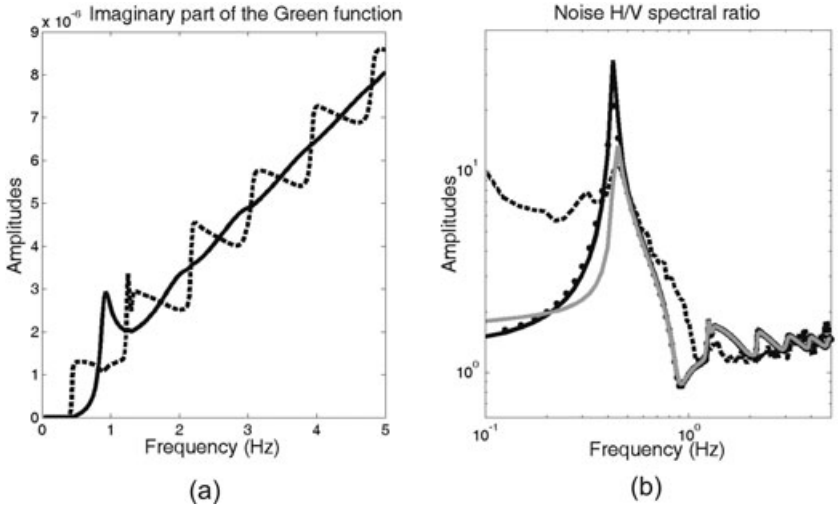

Figure 4. (Left-hand side) Imaginary part of Green's tensor components for both source and receiver at the free surface. Dashed and continuous lines represent $\mathrm{Im}G_{11}$ and $\mathrm{Im}G_{33}$, respectively. (Right-hand side) H/V for stabilized average spectra of 40 s long windows recorded at the Texcoco site (dashed line). The theoretical result of eq. (4) is shown with a continuous grey line. For reference we added the theoretical results of our calculations; with continuous black line for potentials without damping ($Q^{-1} = 0$) and with black dots for the results using generalized modes (Margerin 2009). Two values of *P*-wave velocity were considered $\alpha = 400$ and 800 m s^{-1}, and the computed values are almost equal. At the scale of plot no differences are appreciated. For more details see the text.

based upon a recent study on the energy partitions among waves types (Sánchez-Sesma *et al.* 2011).

Fig. 4 also displays the noise H/V ratio for the Texcoco data. A clear peak at 0.47 Hz is evident with a minor peak at about 0.3 Hz, which suggests a more complex, perhaps deeper structure. For 1–5 Hz, the ratio fluctuates around a value of about 1.4. The result of our theory comes after applying eq. (4) and is also depicted in Fig. 4 for the properties given above (grey line) and assuming no damping ($Q^{-1} = 0$ with black line). For this latter case the results using Margerin's (2009) approach are displayed as well (with black dots). Note that all theoretical values have adequate asymptotic values for both higher and lower frequencies. For frequencies lower than 0.3 Hz the measured H/V ratio displays large values that we are unable to explain at this moment. Perhaps, these ratios reveal a physical feature not accounted for in our modelling. The qualitative agreement of data and model (for $Q = 100$) is remarkable between 0.3 and 5 Hz. The amplitude is somewhat smaller but is acceptable considering that a more detailed calculation is still to be made with more realistic soil models. Note that the peak amplitude in our theory comes from the ratio of the broad peak of $2\mathrm{Im}G_{11}$ and the emerging $\mathrm{Im}G_{33}$.

Our theoretical results display the characteristics that are being commonly used to invert soil structures from H/V: (1) they recover the fundamental resonance frequency of the transfer function for vertical body *S* waves, and (2) they show a strong decay close to the first minimum of the ellipticity of Rayleigh wave. As shown by Konno & Ohmachi (1998) this minimum is located approximately at the double of the frequency of the first maximum for many soils. Malischewsky & Scherbaum (2004) established when the Rayleigh-wave ellipticity yields the shear wave resonance (namely for sufficiently high impedance contrast) and when not. At higher frequencies the theoretical solution displays small peaks related to higher modes (see Fäh *et al.* 2001).

10 DISCUSSION AND CONCLUSIONS

From these results three implications emerge regarding the diffuse nature of microtremor wave fields: (1) the stabilization of the normalized average autocorrelation for a given energy level suggests that the resulting illumination is totally or partially equipartitioned, thus (2) the resulting spectra can be regarded as specific 3-D signatures of the site, and (3) the NHV can be expressed in terms of a quotient that includes the imaginary part of GF components at the source. Our formulation naturally allows for the inversion of the Nakamura's (1989) ratio. The GF includes all the contributions of Rayleigh, Love and body waves. We are currently investigating to what extent partial equipartition and attenuation limit our approach. We expect that using this scheme the residuals in inversion become smaller than those for other approaches.

ACKNOWLEDGMENTS

The authors thank P.-Y. Bard, M. Feriche, K. Irikura, H. Kawase, S. Matsushima, R. Snieder, K. Wapenaar and T. Yokoi for enlightening discussions, M. E. Olson for the careful reading of manuscript and useful suggestions and T. Hirokawa for some calculations; G. Sánchez N. and her team from USI-II-UNAM, found useful references. Supports from DGAPA-UNAM, Project IN121709, Mexico; from Project CGL2010–16250, Spain and FEDER are greatly appreciated. This work was completed while FJS-S was on leave as a Visiting Professor at the Disaster Prevention Research Institute (DPRI) of Kyoto University, at Uji, Kyoto, Japan.

REFERENCES

Aki, K., 1988. Local site effects on strong ground motion, in *Earthquake Engineering and Soil Dynamics I –Recent Advances in Ground Motion Evaluation,* pp. 103–155, ed. Von Thun, J. L., Geotech. Special Pub. No. 20, ASCE, New York, NY.

Arai, H. & Tokimatsu, K., 2004. *S*-wave velocity profiling by inversion of microtremor H/V spectrum, *Bull. seism. Soc. Am.,* **94,** 53–63.

Bard, P.-Y., 2008. The H/V technique: capabilities and limitations based on the results of the SESAME project, *Foreword. Bull. Earthq. Eng.,* **6,** 1–2.

Bonnefoy-Claudet, S., Cornou, C., Bard, P.-Y., Cotton, F., Moczo, P., Kristek, J. & Fäh, D., 2006. H/V ratio: a tool for site effects evaluation. Results from 1-D noise simulations, *Geophys. J. Int.,* **167,** 827–837.

Bonnefoy-Claudet, S., Köhler, A., Cornou, C., Wathelet, M. & Bard, P.-Y., 2008. Effects of love waves on microtremor H/V ratio, *Bull. seism. Soc. Am.,* **98**(1), 288–300.

Cadet, H., 2007. Utilisation combinée des méthodes basées sur le bruit de fond dans le cadre du microzonage sismique, *PhD thesis*, Université J. Fourier, Grenoble.

Cadet, H., Bard, P.-Y. & Rodriguez-Marek, A., 2010. Defining a standard rock site: propositions based on the KiK-net database, *Bull. seism. Soc. Am.,* **100,** 172–195.

Campillo, M. & A. Paul 2003. Long range correlations in the seismic coda, *Science,* **299,** 547–549.

Fäh, D., Kind, F. & Giardini, D., 2001. A theoretical investigation of average H/V ratios, *Geophys. J. Int.,* **145,** 535–549.

Herat, M. 2008. Model HVSR: a Matlab® tool to model horizontal-to-vertical spectral ratio of ambient noise, *Comput. Geosci.,* **34,** 1514–1526.

Knopoff, L., 1964. A matrix method for elastic wave problems, *Bull. seism. Soc. Am.,* **54,** 431–438.

Konno, K. & Ohmachi, T., 1998. Ground-motion characteristics estimated from spectral ratio between horizontal and vertical components of microtremor, *Bull. seism. Soc. Am.,* **88,** 228–241.

Lermo, J. & Chávez-García, F.J., 1994. Are microtremors useful in site response evaluation? *Bull. seism. Soc. Am.,* **84,** 1350–1364.

Lunedei, E. & Albarello, D., 2010. Theoretical HVSR curves from full wavefield modelling of ambient vibrations in a weakly dissipative layered Earth, *Geophys. J. Int.,* **181,** 1093–1108, doi:10.1111/j.1365-246X.2010.04560.x

Malischewsky, P.G. & Scherbaum, F., 2004. Love's formula and H/V-ratio (ellipticity) of Rayleigh waves, *Wave Motion,* **40,** 57–67.

Margerin, L., 2009. Generalized eigenfunctions of layered elastic media and application to diffuse fields, *J. acoust. Soc. Am.,* **125**(1), 164–174.

Margerin, L., Campillo, M., van Tiggelen, B.A. & Hennino, R., 2009. Energy partition of seismic coda waves in layered media: theory and application to Pinyon Flats Observatory, *Geophys. J. Int.,* **177,** 571–585.

Nakamura, Y., 1989. A method for dynamic characteristics estimation of subsurface using microtremor on the ground surface, *Q. Rep. Railw. Tech. Res. Inst.,* **30,** 25–30.

Nakamura, Y., 2000. Clear identification of fundamental idea of Nakamura's technique and its applications, in *Proceedings of 12th World Conf. on Earthq. Eng.,* New Zealand, 8 pp, (CD-ROM).

Perton, M., Sánchez-Sesma, F.J., Rodríguez-Castellanos, A., Campillo, M. & Weaver, R. L., 2009. Two perspectives on equipartition in diffuse elastic fields in three dimensions, *J. acoust. Soc. Am.,* **126,** 1125–1130.

Pilz, M., Parolai, S., Leyton, F., Campos, J. & Zschau, J., 2009. A comparison of site response techniques using earthquake data and ambient seismic noise analysis in the large urban areas of Santiago de Chile, *Geophys. J. Int.,* **178**(2), 713–728.

Sánchez-Sesma, F.J., 1987. Site effects on strong ground motion, *Soil Dyn. Earthq. Eng.,* **6,** 124–132.

Sánchez-Sesma, F.J. & Campillo, M., 2006. Retrieval of the Green function from cross-correlation: the canonical elastic problem, *Bull. seism. Soc. Am.,* **96,** 1182–1191.

Sánchez-Sesma, F. J., Pérez-Ruiz, J. A., Campillo, M. & Luzón, F., 2006. The elastodynamic 2D Green function retrieval from cross-correlation: the canonical inclusion problem, *Geophys. Res. Lett.,* **33,** L13305, doi:10.1029/2006 GL026454.

Sánchez-Sesma, F.J., Pérez-Ruiz, J.A., Luzón, F., Campillo, M. & Rodríguez-Castellanos, A., 2008. Diffuse fields in dynamic elasticity, *Wave Motion,* **45,** 641–654.

Sánchez-Sesma, F. J., Rodríguez, M., Iturrarán-Viveros, U., Rodríguez-Castellanos, A., Suarez, M., Santoyo, M. A., García-Jerez, A. & Luzón, F., 2010. Site effects assessment using seismic noise, in *Proceedings of the 9th International Workshop on Seismic Microzoning and Risk Reduction,* 2010, February 21–24, Cuernavaca, Mexico.

Sánchez-Sesma, F. J., Weaver, R. L., Kawase, H., Matsushima, S., Luzón, F. & Campillo, M., 2011. Energy partitions among elastic waves for dynamic surface loads in a semi-infinite solid, *Bull. seism. Soc. Am.,* doi:10.1785/0120100196, in press.

Sato, H., 2010. Retrieval of Green's function having coda waves from the cross-correlation function in a scattering medium illuminated by a randomly homogeneous distribution of noise sources on the basis of the first-order Born approximation, *Geophys. J. Int.,* **180,** 759–764.

Weaver, R.L., 1982. On diffuse waves in solid media, *J. acoust. Soc. Am.,* **71,** 1608–1609.

Weaver, R.L., 1985. Diffuse elastic waves at a free surface, *J. acoust. Soc. Am*., **78,** 131–136.

Weaver, R.L. & Lobkis, O.I., 2004. Diffuse fields in open systems and the emergence of the Green's function, *J. acoust. Soc. Am.,* **116,** 2731–2734.

Yokoi, T. & Margaryan, S., 2008. Consistency of the spatial autocorrelation method with seismic interferometry and its consequence, *Geophys. Prospect.,* **56,** 435–451.

SUPPORTING INFORMATION

Additional Supporting Information may be found in the online version of this article:

Appendix S1. Appendix to 'Data Processing'.
Appendix S2. Appendix to 'The Imaginary Part of Green's Function at the Surface Load Point. The Layered 3-D Elastic Case'.

Please note: Wiley-Blackwell are not responsible for the content or functionality of any supporting materials supplied by the authors. Any queries (other than missing material) should be directed to the corresponding author for the article.